AMERICAN SOCIETY FOR MICROBIOLOGY | Molecular and Cellular Biology®

RESEARCH ARTICLE

Defective Flux of Thrombospondin-4 through the Secretory Pathway Impairs Cardiomyocyte Membrane Stability and Causes Cardiomyopathy

Matthew J. Brody,[a] Davy Vanhoutte,[a] Tobias G. Schips,[a] Justin G. Boyer,[a,b] Chinmay V. Bakshi,[a] Michelle A. Sargent,[a,b] Allen J. York,[a,b] Jeffery D. Molkentin[a,b]

[a]Department of Pediatrics, Cincinnati Children's Hospital Medical Center, Cincinnati, Ohio, USA
[b]Howard Hughes Medical Institute, Cincinnati, Ohio, USA

ABSTRACT Thrombospondins are stress-inducible secreted glycoproteins with critical functions in tissue injury and healing. Thrombospondin-4 (Thbs4) is protective in cardiac and skeletal muscle, where it activates an adaptive endoplasmic reticulum (ER) stress response, induces expansion of the ER, and enhances sarcolemmal stability. However, it is unclear if Thbs4 has these protective functions from within the cell, from the extracellular matrix, or from the secretion process itself. In this study, we generated transgenic mice with cardiac cell-specific overexpression of a secretion-defective mutant of Thbs4 to evaluate its exclusive intracellular and secretion-dependent functions. Like wild-type Thbs4, the secretion-defective mutant upregulates the adaptive ER stress response and expands the ER and intracellular vesicles in cardiomyocytes. However, only the secretion-defective Thbs4 mutant produces cardiomyopathy with sarcolemmal weakness and rupture that is associated with reduced adhesion-forming glycoproteins in the membrane. Similarly, deletion of *Thbs4* in the *mdx* mouse model of Duchenne muscular dystrophy enhances cardiomyocyte membrane instability and cardiomyopathy. Finally, overexpression of the secretion-defective Thbs4 mutant in *Drosophila*, but not wild-type Thbs4, impaired muscle function and sarcomere alignment. These results suggest that transit through the secretory pathway is required for Thbs4 to augment sarcolemmal stability, while ER stress induction and vesicular expansion mediated by Thbs4 are exclusively intracellular processes.

KEYWORDS cardiomyopathy, heart, thromobospondin, transgenic mice

Cardiomyocytes are structurally connected to the myocardial extracellular matrix (ECM) through sarcolemmal glycoproteins, including sarcoglycans, dystroglycans, and integrins, which provide mechanical and structural stability to the sarcolemma during contraction or during stress stimulation (1–7). Molecular mechanisms underlying cardiac ECM remodeling and turnover, as well as the manner in which the attachment cytoskeletal glycoproteins are regulated in content, membrane cycling, and assembly, remain largely unknown.

Thrombospondins (Thbs) are a family of secreted oligomeric glycoproteins that are induced in response to tissue injury (8–11). There are five mammalian Thbs genes that are divided into two subgroups based on protein structure and oligomerization state, with Thbs1 and Thbs2 forming trimers while Thbs3, Thbs4, and Thbs5 form pentamers. Thbs1 and Thbs2 uniquely contain a type I repeat domain involved in transforming growth factor β (TGF-β) signaling, as well as a region that can regulate angiogenesis (8–11). The evolutionarily more ancient Thbs proteins, Thbs3, Thbs4, and Thbs5/cartilage oligomeric matrix protein (COMP), lack the type I repeat (T1R) region but contain ubiquitously shared epidermal growth factor (EGF)-like repeats, type III repeats (T3R), and the L-type lectin (TSP-C) domain (9, 12–14). Importantly, DXDXDG calcium

Received 6 March 2018 **Returned for modification** 30 March 2018 **Accepted** 18 April 2018

Accepted manuscript posted online 30 April 2018

Citation Brody MJ, Vanhoutte D, Schips TG, Boyer JG, Bakshi CV, Sargent MA, York AJ, Molkentin JD. 2018. Defective flux of thrombospondin-4 through the secretory pathway impairs cardiomyocyte membrane stability and causes cardiomyopathy. Mol Cell Biol 38:e00114-18. https://doi.org/10.1128/MCB.00114-18.

Address correspondence to Jeffery D. Molkentin, jeff.molkentin@cchmc.org.

binding motifs within the T3R domains of the Thbs proteins are critical for their flux through the secretory pathway and deposition briefly outside the cell (15–19). For example, mutations in calcium binding sites in the T3R domains of the human Thbs5/COMP gene cause skeletal dysplasia, including pseudoachondroplasia (PSACH) and multiple epiphyseal dysplasia (MED) (15, 16, 20–25). These mutations result in mutant Thbs5 proteins that accumulate in the endoplasmic reticulum (ER) and have delayed secretion, resulting in defective chondrocytes and altered ECM composition (15–18, 22, 23, 26, 27). Similarly, we have shown that mutation of DXDXDG calcium binding sites within the T3R domains of Thbs4 results in a loss of secretion by cultured cardiomyocytes, in contrast to the robustly secreted wild-type Thbs4 protein (19).

The Thbs proteins regulate the molecular composition of the ECM in response to tissue injury and tissue healing (8, 11, 28), which was always presumed to occur from outside the cells. However, recent studies showed that Thbs can have an intracellular function involving vesicular trafficking or chaperoning of structural plasma membrane and ECM proteins during the tissue injury and healing response, in part by directly upregulating the activity of activating transcription factor 6α (Atf6α) (11, 19, 29). Specifically, Thbs4 upregulates vesicular trafficking of dystroglycans and sarcoglycans in myocytes, resulting in enhanced membrane stability and preservation of myocyte-ECM attachments (29). Indeed, overexpression of Thbs4 protects the heart in genetic models of cardiomyopathy and surgical models of cardiac pressure overload and myocardial infarction injury, as well as reduces pathology and deterioration of muscle function in multiple models of muscular dystrophy that are characterized by a weakened sarcolemma (11, 29).

Thbs4 is transiently present in the ECM but is taken up via endocytosis (29, 30), suggesting that intracellular flux of Thbs4 through the secretory pathway, its transient residence in the ECM, and its reuptake may be integral for its molecular functions. In this study, we generated mice with cardiac cell-specific overexpression of a secretion-defective mutant of Thbs4 to investigate the role that its secretion plays in the cardioprotective functions of this protein. We determined that overexpression of a secretion-defective mutant of Thbs4 in transgenic mice actually causes cardiomyopathy, despite having the same ability to induce ER stress and intracellular vesicular expansion as wild-type Thbs4.

RESULTS

Mutation of aspartic acid residues in DXDXDG calcium binding sites within the T3R domains of the gene for human Thbs5/COMP, a highly homologous family member of Thbs4, results in the bone growth and development disorders PSACH and MED and in delayed secretion or increased retention of Thbs5/COMP protein in the ER of chondrocytes (15–17, 21, 24–27). To interrogate the functions of mouse Thbs4 in the secretory pathway, we generated a Thbs4 construct with mutations in 6 of the consensus DXDXDG calcium binding sites within the T3R domains (Fig. 1A). We generated recombinant adenoviruses for wild-type Thbs4 or Thbs4-mCa^{2+} with a C-terminal Flag tag or β-galactosidase (βgal) as a control to transduce cultured neonatal cardiomyocytes for analysis of these proteins. Importantly, mutation of these calcium binding sites in Thbs4 did not alter its pentameric structure, which was similar to that of wild-type Thbs4 as analyzed by SDS-PAGE under reducing and nonreducing conditions from adenovirus-infected neonatal cardiomyocyte protein extracts (Fig. 1B). We concentrated medium and harvested intracellular extracts from cardiomyocytes overexpressing wild-type Thbs4 or the Thbs4-mCa^{2+} mutant; immunoblotting revealed abundant intracellular expression of both proteins, but only wild-type Thbs4 was secreted into the medium (Fig. 1C). Secretion of atrial natriuretic factor (ANF) was not compromised by the Thbs4-mCa^{2+} mutant but in fact was increased to the same extent as overexpression of wild-type Thbs4 (Fig. 1C), consistent with the known ability of Thbs4 to enhance intracellular vesicular trafficking and generalized secretion in cardiomyocytes (11, 29).

Thbs4 is known to mediate an adaptive ER stress response and expansion of the ER and intracellular vesicles mediated through its interaction with activating transcription

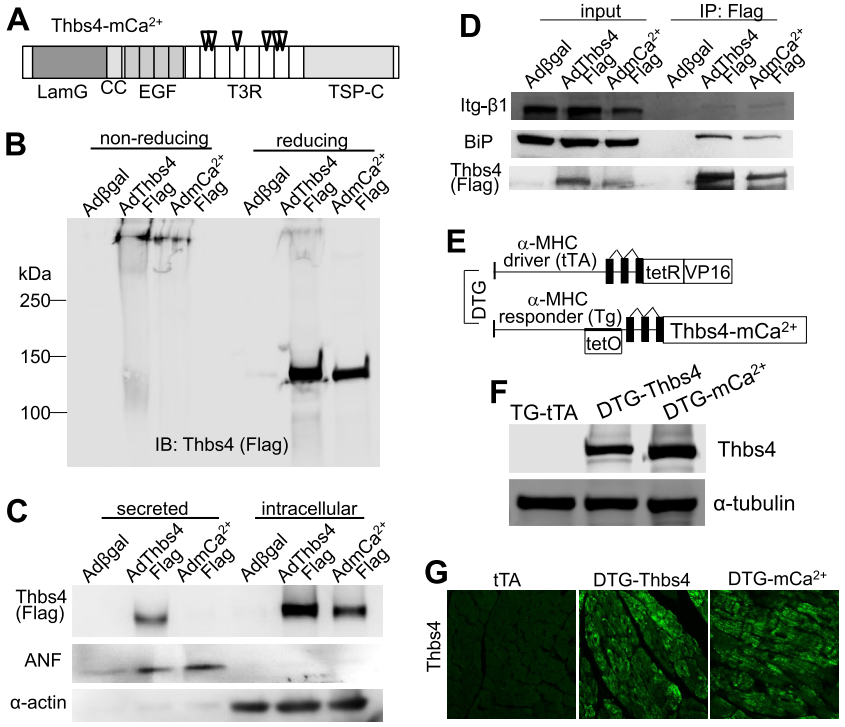

FIG 1 Generation of transgenic mice with cardiac cell-specific overexpression of a secretion-defective mutant of thrombospondin-4. (A) Schematic diagram depicting the secretion-defective mutant of thrombospondin-4 (Thbs4-mCa^{2+}). The 6 arrowheads in the T3R domains of Thbs4 indicate sites of mutagenesis of DXDXDG calcium binding motifs to AXAXAG. Other abbreviations: LamG, laminin-G domain; CC, coiled-coil oligomerization domain; EGF, epidermal growth factor-like repeat domains; T3R, type III repeat domains; TSP-C, C-terminal L-type lectin domain. (B) Western blotting for Thbs4 under reducing or nonreducing conditions using lysates from neonatal rat ventricular cardiomyocytes (NRVMs) with adenovirus-mediated overexpression of β-galactosidase (βgal), wild-type Thbs4, or Thbs4-mCa^{2+}. (C) Western blotting of cultured media or intracellular lysates of NRVMs transduced with recombinant adenovirus to overexpress βgal, wild-type Thbs4, or Thbs4-mCa^{2+}. Atrial natriuretic factor (ANF) and sarcomeric α-actin were used as secreted or intracellular protein positive controls, respectively. (D) Thbs4 was immunoprecipitated (IP) from lysates of NRVMs transduced with adenoviruses to overexpress wild-type Thbs4 or Thbs4-mCa^{2+} and immunoblotted for the Thbs4 interactors BiP and integrin β1 (Itg-β1). (E) Schematic of the binary transgenic system used to overexpress Thbs4-mCa^{2+} in the heart. (F and G) Western blotting (F) and immunohistochemistry (G) for Thbs4 in hearts of transgenic mice overexpressing wild-type Thbs4 (DTG-Thbs4) or Thbs4-mCa^{2+} (DTG-mCa^{2+}). α-Tubulin was used as a loading control.

factor 6α (Atf6α) (11, 19). Our previous studies showed that just like wild-type Thbs4, the mCa^{2+} mutant is able to interact with Atf6α (19). Thbs4 also interacts with integrin β1 (9, 29) and the ER chaperone BiP (Grp78) (19) in cardiomyocytes, so we also tested whether these interactions were dependent on the calcium binding sites within the T3R domain. The results showed that both the wild type and the secretion-defective Thbs4 mutant interact with integrin β1 and BiP in cardiomyocytes (Fig. 1D). Taken together, these data indicate that the Thbs4-mCa^{2+} mutant properly folds and oligomerizes in the ER and interacts with Thbs4 binding partners but is defective in its secretory activity.

We previously generated inducible binary transgenic mice with cardiac tissue-specific overexpression of wild-type Thbs4, which resulted in animals that were protected from cardiomyopathy-promoting insults (11). In this study, we generated transgenic mice overexpressing the Thbs4-mCa^{2+} mutant in the heart using the same binary inducible genetic system in which one transgene expresses the tetracycline transactivator (tTA) protein from the α-myosin heavy chain (α-MHC) promoter and the other transgene contains the *tet* operator embedded within a modified α-MHC promoter (31). Double transgenic mice (DTG-mCa^{2+}) containing both the tTA and Thbs4-mCa^{2+} transgenes express the secretion-defective mCa^{2+} Thbs4 mutant in the heart in the absence of tetracycline or doxycycline (32) (Fig. 1E). Western blotting (Fig. 1F) and

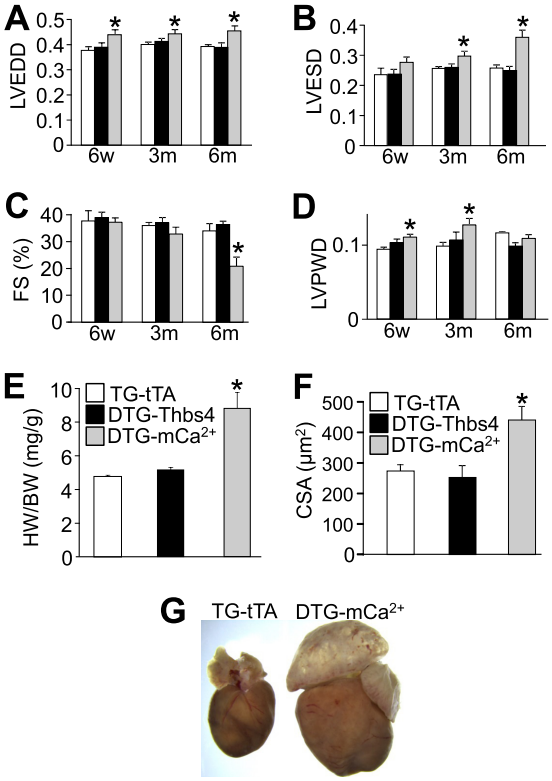

FIG 2 Cardiomyopathy in transgenic mice with cardiac tissue-specific overexpression of the secretion-defective mutant of Thbs4. (A to D) Echocardiography was performed to evaluate cardiac structure and function in cardiac tissue-specific transgenic mice overexpressing wild-type Thbs4 (DTG-Thbs4) or the secretion-defective mutant of Thbs4 (DTG-mCa^{2+}) and single transgenic tTA controls (TG-tTA) at the indicated age. Abbreviations: LVEDD, left ventricular end-diastolic dimension; LVESD, left ventricular end-systolic dimension; LVPWD, left ventricular posterior wall thickness; FS, fractional shortening; w, weeks; m, months. Measurements in panels A, B, and D are in centimeters. (E and F) Ratios of heart weight (HW) to body weight (BW) (E) and cell surface area (CSA) measurements (F) from cardiac histological sections of transgenic mice at 2 months of age. (G) Gross morphology of hearts of DTG-mCa^{2+} and littermate TG-tTA mice at 2 months of age. *, $P < 0.05$ versus the value for TG-tTA controls.

immunohistochemistry of cardiac sections (Fig. 1G) demonstrated robust expression of the secretion-defective Thbs4 mutant protein, similar to levels of Thbs4 in wild-type DTG mice. Although wild-type Thbs4 is secreted by cardiomyocytes *in vitro* (Fig. 1C), it is rapidly taken up by endocytosis and thus not observed *in vivo* within the ECM of the heart or skeletal muscle (11, 19, 29). Indeed, as we reported previously (11, 29), overexpression of wild-type Thbs4 in the heart results in predominantly intracellular localization of this protein, similar to the case with mutant Thbs4 protein (Fig. 1G).

To evaluate the effects of blockade of Thbs4 secretion on cardiac structure and function, we performed echocardiography on DTG-mCa^{2+} mice along with DTG mice overexpressing wild-type Thbs4 in the heart (DTG-Thbs4) (11) and tTA single transgenic controls. The results demonstrate normal cardiac structure and function in DTG-Thbs4 mice (Fig. 2A to E). However, DTG-mCa^{2+} mice develop cardiac dilation characterized by enlargement of the left ventricular chamber (Fig. 2A and B), heart failure characterized by reduced fractional shortening of the left ventricle (Fig. 2C), and cardiac hypertrophy characterized by increased thickness of the left ventricular free wall, increased heart weight normalized to body weight, and increased cardiomyocyte cell surface area (CSA) (Fig. 2D to F). Gross morphological analyses of hearts at 2 months of age confirmed the cardiomyopathic phenotype of the DTG-mCa^{2+} mice with atrial dilation and clotting (Fig. 2G). These data indicate that overexpression of Thbs4 containing mutations in residues required for its secretory activity induces cardiomyopathy, in stark contrast to the cardioprotective effects imparted by overexpression of wild-type Thbs4 (11).

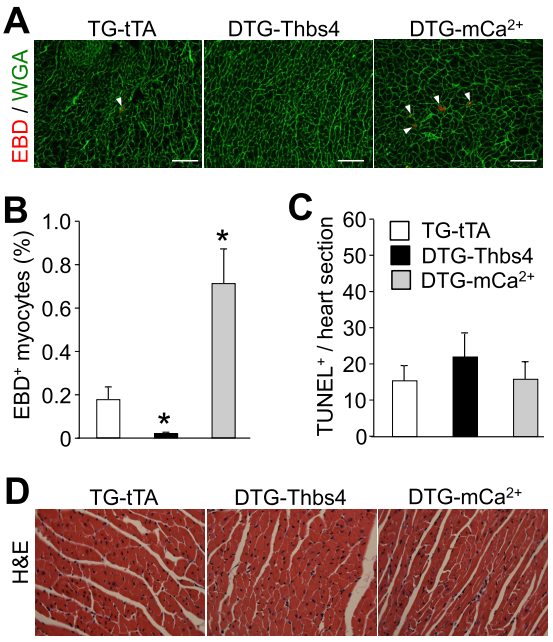

FIG 3 Cardiomyocyte membrane damage in hearts overexpressing secretion-defective Thbs4. Evans blue dye (EBD) uptake was evaluated in hearts of transgenic mice overexpressing wild-type (DTG-Thbs4) or secretion-defective Thbs4 (DTG-mCa^{2+}) and TG-tTA controls at 2 months of age. (A and B) Representative images (A) and quantification (B) of cardiomyocyte EBD uptake from heart histological sections of transgenic mice of the indicated genotypes. Membranes were stained with wheat germ agglutinin (WGA), in green. Arrowheads indicate EBD-positive myocytes (red fluorescence). Scale bars = 100 μm. (C) Quantification of TUNEL-positive cells from cardiac sections of transgenic mice of the indicated genotypes. (D) H&E staining of cardiac histological tissue sections from the indicated mice at 2 months of age. *, $P < 0.05$ versus the value for TG-tTA controls.

In skeletal muscle, Thbs4 protects from muscular dystrophy in association with increased intracellular vesicular trafficking, enhancement of plasma membrane stability, and greater membrane attachment complexes (29). We thus hypothesized that inhibition of Thbs4 secretion might decrease cardiomyocyte sarcolemmal stability. To examine this hypothesis, we injected 2-month-old mice with Evans blue dye (EBD), a membrane-impermeable dye that binds albumin and can reveal cells with ruptured or leaky membranes *in vivo* (33). Hearts were harvested 2 days following injection, cryosectioned, and imaged for EBD$^+$ cardiomyocytes. We observed a significant increase of EBD$^+$ cardiomyocytes in hearts from DTG-mCa^{2+} mice (Fig. 3A and B), indicating that overexpression of the secretion-defective mutant weakens the sarcolemma *in vivo*. In contrast, overexpression of wild-type Thbs4 resulted in a significant reduction of baseline EBD$^+$ cardiomyocytes compared with the amount in control mice (Fig. 3A and B). EBD positivity was not associated with alterations in apoptosis or necrosis as detected by terminal deoxynucleotidyltransferase-mediated dUTP-biotin nick end labeling (TUNEL) staining (Fig. 3C) and histological evaluation of hematoxylin and eosin (H&E)-stained cardiac sections (Fig. 3D). Thus, cardiomyopathy in mice with cardiac tissue-specific overexpression of the secretion-defective Thbs4-mCa^{2+} mutant is associated with enhanced sarcolemmal damage, while transgenic mice with overexpression of wild-type Thbs4 have slightly better sarcolemmal stability, as we previously observed in skeletal muscle (29).

To further evaluate the effects of Thbs4 on cardiomyocyte sarcolemmal integrity, we investigated the *mdx* model of Duchenne muscular dystrophy, which is a model with known instability of the sarcolemma that ultimately results in dystrophic cardiomyopathy in aged mice (34, 35). We have previously shown that skeletal muscle from *mdx* mice induces Thbs4 protein (29), and in this study, we observed that hearts of *mdx* mice also upregulate Thbs4 protein (Fig. 4A), likely as a compensatory mechanism directed at healing. Given this upregulation, we crossed mice in which the Thbs4 gene had been

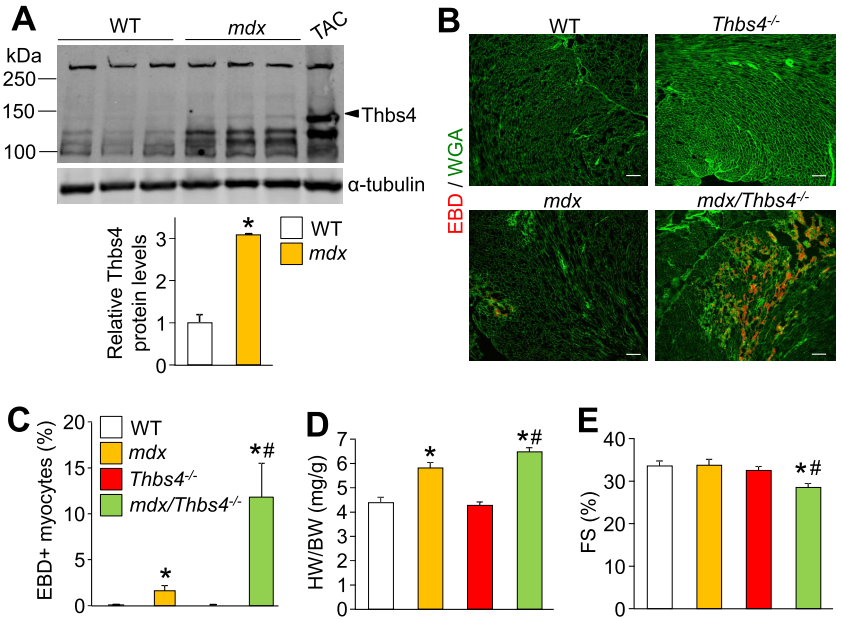

FIG 4 Thrombospondin-4 protects from dystrophic cardiomyopathy. (A) Western blotting and quantitation (lower portion) of Thbs4 protein in hearts of *mdx* mice at 3 months of age. Lysate from a pressure overloaded mouse heart (TAC) was used as a positive control. (B and C) Evans blue dye (EBD; red fluorescence) uptake was evaluated in hearts of *Thbs4*$^{-/-}$ mice crossed to *mdx* mice at 2 months of age. The data show representative histochemical images and quantification of cardiomyocyte EBD uptake in cardiac histological sections of mice of the indicated genotypes at 2 months of age. Membranes were stained with wheat germ agglutinin (green fluorescence), and EBD^{+} cells show red fluorescence. Scale bar = 100 μm. (D and E) Ratios of heart weight to body weight (D) and percent fractional shortening (FS) (E) as evaluated by echocardiography in mice of the indicated genotypes at 1 year of age. *, $P < 0.05$ versus the value for the wild type (WT); #, $P < 0.05$ versus the value for *mdx* mice.

deleted (*Thbs4*$^{-/-}$) with *mdx* mice and evaluated cardiomyocyte membrane permeability with the Evans dye uptake assay at 2 months of age, which is prior to cardiac disease development in *mdx* mice (36–38). Remarkably, deletion of *Thbs4* enhanced cardiomyocyte membrane permeability in the *mdx* background (Fig. 4B and C), again indicating that Thbs4 has critical functions dedicated to membrane stability. Consistent with the greater potential disease profile of the weakened sarcolemma in *Thbs4*$^{-/-}$/*mdx* mice, we observed increased cardiac hypertrophy (Fig. 4D) and decreased cardiac function (Fig. 4E) with aging compared to *mdx* mice alone. Taken together, these data demonstrate that the absence of *Thbs4* in the *mdx* dystrophic background results in greater cardiomyopathy because Thbs4 normally serves as a protective healing factor in the heart during this disease.

Previous work has demonstrated that Thbs4 induces an adaptive ER stress response as well as upregulation of ER-to-Golgi trafficking in the heart and skeletal muscle (11, 29). To determine if the secretion-defective Thbs4 mutant is similarly able to modulate the ER stress response and induction of anterograde trafficking, we performed Western blotting in cardiac lysates from transgenic mice at 2 months of age. Results demonstrate that similar to the case with wild-type Thbs4, overexpression of the Thbs4-mCa^{2+} mutant induces an adaptive ER stress response, including upregulation of BiP, protein disulfide isomerase (PDI), calreticulin (Calret), and Armet (also known as mesencephalic astrocyte-derived neurotrophic factor [MANF]) (Fig. 5A and B). The Thbs4-mCa^{2+} mutant also robustly induces ER-to-Golgi trafficking factors, including the GTPases SAR1, Rab6, and Rab24 (Fig. 5C and D), which may be an attempt to cope with defective flux of glycoproteins chaperoned by Thbs4 or defective flux of Thbs4 itself through the secretory pathway. Thus, despite the lack of flux through the secretory pathway and temporary release outside the cell, the Thbs4-mCa^{2+} mutant acts identically to wild-type Thbs4 in upregulating proteins involved in the ER stress response and intracellular anterograde trafficking through the secretory pathway (29).

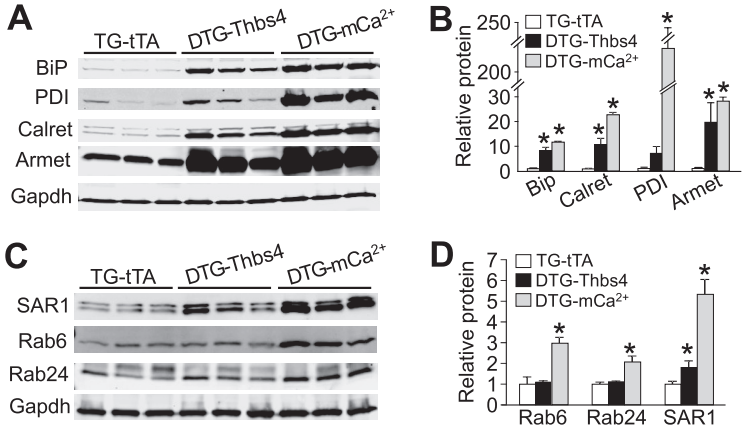

FIG 5 Induction of the adaptive ER stress response and secretory pathway proteins in hearts overexpressing wild-type Thbs4 or the secretion-defective Thbs4 mutant. (A and C) Western blotting for ER stress response (A) and ER-to-Golgi trafficking (C) proteins in transgenic hearts overexpressing wild-type Thbs4 (DTG-Thbs4) or the secretion-defective Thbs4 mutant (DTG-mCa^{2+}). Protein levels in panels A and C are quantified in panels B and D, respectively. Abbreviations: PDI, protein disulfide isomerase; Calret, calreticulin. $n = 3$. *, $P < 0.05$ versus the value for TG-tTA mice.

Thbs4 also induces an unprecedented and dramatic expansion of ER in both heart and skeletal muscle (11, 29) that is mediated through Atf6α (19, 29). To evaluate whether the Thbs4-mCa^{2+} mutant is also capable of expanding ER/intracellular vesicles *in vivo*, we performed electron microscopy on hearts from these transgenic mice versus wild-type Thbs4 and tTA controls at 2 months of age. Results reveal normal cardiac ultrastructure in tTA control mouse hearts but a profound expansion of ER in hearts overexpressing the wild type or the Thbs4-mCa^{2+} mutant (Fig. 6A). An even greater expansion of intracellular vesicles was observed in hearts overexpressing the Thbs4-mCa^{2+} mutant compared to those overexpressing wild-type Thbs4 (Fig. 6A), which could be due to greater retention and reduced trafficking speed of this Thbs4 mutant through the ER and post-ER vesicles or an effort to bolster secretory pathway through-

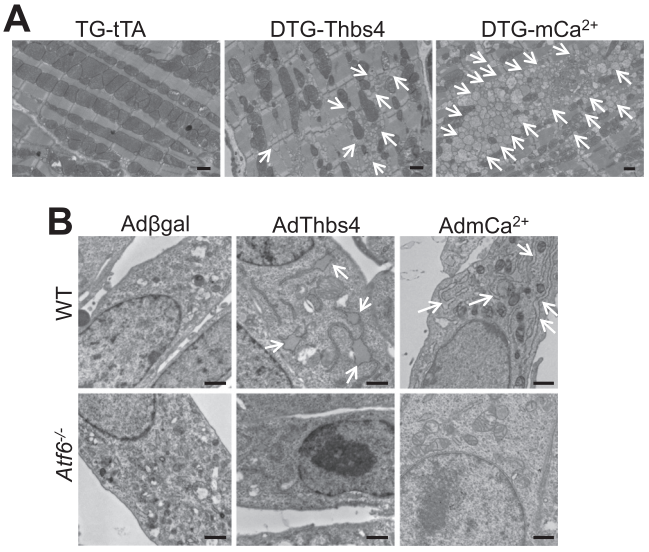

FIG 6 Wild-type Thbs4 and the secretion-defective Thbs4 mutant induce Atf6α-dependent ER expansion. (A) Electron microscopy of hearts from transgenic mice overexpressing wild-type Thbs4 (DTG-Thbs4) or the secretion-defective Thbs4 mutant (DTG-mCa^{2+}). Arrows indicate expanded ER and intracellular vesicles. Scale bars = 1 μm. (B) Electron microscopy of wild-type or *Atf6*$^{-/-}$ MEFs with adenoviral overexpression of wild-type Thbs4 (AdThbs4), the secretion-defective Thbs4 mutant (AdmCa^{2+}), or β-galactosidase as a control (Adβgal). Scale bars = 1 μm. Arrows indicate expanded ER and intracellular vesicles.

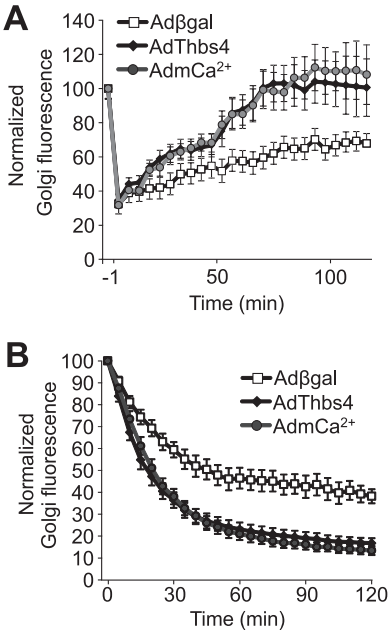

FIG 7 Wild-type Thbs4 and the secretion-defective mutant enhance global secretory pathway flux in cardiomyocytes. Shown are time courses of GalNac-T2-RFP (A) and VSVG-eGFP (B) fluorescence changes in cultured rat neonatal cardiomyocytes transduced with adenoviruses to overexpress wild-type Thbs4, the secretion-defective Thbs4 mutant (mCa^{2+}), or β-galactosidase as a control. Change in fluorescence after FRAP (A) or iFRAP (B) was used to assess ER-to-Golgi or Golgi-to-plasma membrane trafficking, respectively. Averaged data from four independent experiments with similar results are shown.

put to try to normalize sarcolemmal instability. To determine if vesicular expansion is also mediated through the activity of Atf6α, we transduced wild-type mouse embryonic fibroblasts (MEFs) and MEFs with deletion of the *Atf6* gene (encodes Atf6α protein) (*Atf6*$^{-/-}$) with adenoviruses to overexpress wild-type Thbs4 or the Thbs4-mCa^{2+} mutant and evaluated ultrastructure by electron microscopy. As expected, wild-type Thbs4 induced a dramatic expansion of the ER in wild-type MEFs, which was abrogated in *Atf6*$^{-/-}$ MEFs (19) (Fig. 6B). Similarly, overexpression of the Thbs4-mCa^{2+} mutant resulted in prominent ER expansion in wild-type MEFs that was not evident in *Atf6*$^{-/-}$ MEFs (Fig. 6B), demonstrating that both the wild type and the secretion-defective Thbs4 mutant mediate Atf6α-dependent expansion of the ER.

We previously demonstrated that Thbs4 enhances both ER-to-Golgi and Golgi-to-plasma membrane vesicular trafficking in cardiomyocytes in an Atf6α-dependent manner (29). We evaluated ER-to-Golgi trafficking in cultured neonatal cardiomyocytes with adenovirus-mediated overexpression of the wild type or the Thbs4-mCa^{2+} mutant by coinfecting baculovirus to overexpress GalNAcT2-RFP, a red fluorescent protein (RFP)-tagged Golgi resident protein, and then performing fluorescence recovery after photobleaching (FRAP) to monitor vesicular trafficking. The results indicate that both the wild type and the Thbs4-mCa^{2+} mutant accelerate ER-to-Golgi trafficking (Fig. 7A). Similarly, we evaluated Golgi-to-sarcolemma trafficking by cooverexpressing vesicular stomatitis virus G protein fused to enhanced green fluorescent protein (VSVG-eGFP) and performing inverse FRAP (iFRAP). The data again demonstrate that both the wild type and the Thbs4-mCa^{2+} mutant accelerate Golgi-to-plasma membrane trafficking compared to βgal-transduced controls (Fig. 7B).

Given the increased cardiomyocyte membrane rupture in hearts overexpressing the Thbs4-mCa^{2+} mutant, we examined whether the membrane residency and trafficking of structural sarcolemmal glycoproteins were defective in hearts from DTG-mCa^{2+} mice. We affinity purified membrane glycoproteins from transgenic hearts using wheat germ agglutinin and immunoblotted for sarcoglycans and dystroglycans, structural membrane glycoproteins critically important for maintaining myocyte membrane in-

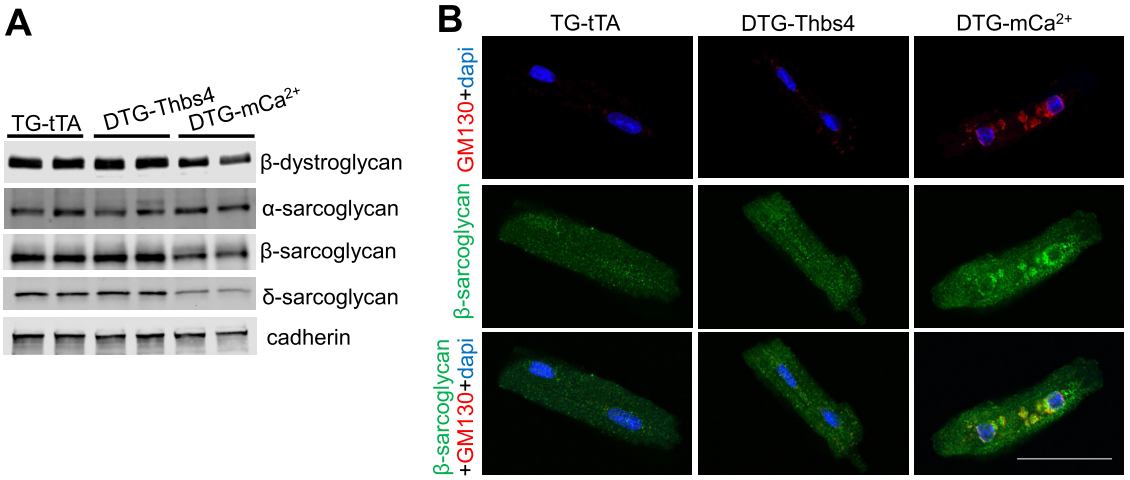

FIG 8 Impaired sarcolemmal glycoprotein trafficking in hearts overexpressing secretion-defective Thbs4. (A) Western blotting for membrane glycoproteins purified from hearts of transgenic mice overexpressing wild-type Thbs4 (DTG-Thbs4) or the secretion-defective mutant (DTG-mCa^{2+}). Cadherin was used as a loading control. (B) Representative experiment of immunocytochemistry for β-sarcoglycan and the Golgi marker GM130 in cardiomyocytes isolated from transgenic hearts of the indicated genotype. Scale bar = 50 μm. Similar results were obtained in 2 additional experiments.

tegrity in cardiac and skeletal muscle myocytes (3, 4, 39). Membrane residency of β-dystroglycan, β-sarcoglycan, and δ-sarcoglycan was reduced in hearts overexpressing the secretion-deficient Thbs4-mCa^{2+} mutant (Fig. 8A), suggesting that impairment of Thbs4 secretion reduces trafficking or plasma membrane insertion of specific structural sarcolemmal glycoproteins. To further investigate the effects of Thbs4 secretory pathway flux on glycoprotein trafficking, we performed immunostaining experiments on cardiomyocytes isolated from transgenic hearts. We found an accumulation of β-sarcoglycan within the Golgi apparatus in hearts from DTG-mCa^{2+} mice as evidenced by colocalization of β-sarcoglycan with GM130 (Fig. 8B). These data indicate that specific glycoprotein trafficking is impaired or delayed by overexpression of the secretion-defective Thbs4 mutant, further supporting the greater mechanism whereby Thbs4 selectively regulates sarcolemmal stability.

To determine if thrombospondins have evolutionarily conserved functions in preserving myocyte structure and function through mechanisms that depend on its secretion, we generated transgenic *Drosophila* flies with skeletal muscle-specific (Mef2-driven) overexpression of the secretion-defective Thbs4 mutant, which we interrogated by Western blotting (Fig. 9A). We have previously shown that overexpression of wild-type Thbs4 in muscle ameliorates deterioration of locomotor function and pathology in a *Drosophila* model of muscular dystrophy (29). In this study, we hypothesized that impairment of Thbs4 secretory activity in *Drosophila* would be deleterious to muscle structure and function. We performed electron microscopy on transgenic flies at 25 days of age, which revealed normal myofiber ultrastructure in control flies and flies overexpressing wild-type Thbs4, but transgenic *Drosophila* overexpressing the secretion-defective Thbs4 mutant in muscle exhibited a dramatic misalignment of sarcomeres and torn myofibers in the indirect flight muscle (Fig. 9B). Indeed, a negative geotaxis assay to evaluate locomotor function in *Drosophila* showed that wild-type Thbs4 overexpression in muscle caused no issues, while flies overexpressing the secretion-defective Thbs4 mutant had progressively impaired muscle function beginning at 5 days of age (Fig. 9C). Thus, overexpression of a secretion-defective Thbs4 mutant impairs muscle structure and function in *Drosophila*, consistent with evolutionarily conserved functions for thrombospondins in mediating vesicular trafficking and maintaining myocyte membrane stability.

DISCUSSION

Thbs4 is upregulated during disease and activates an adaptive ER stress response, expands the ER and intracellular vesicles, and enhances the sarcolemmal abundance of

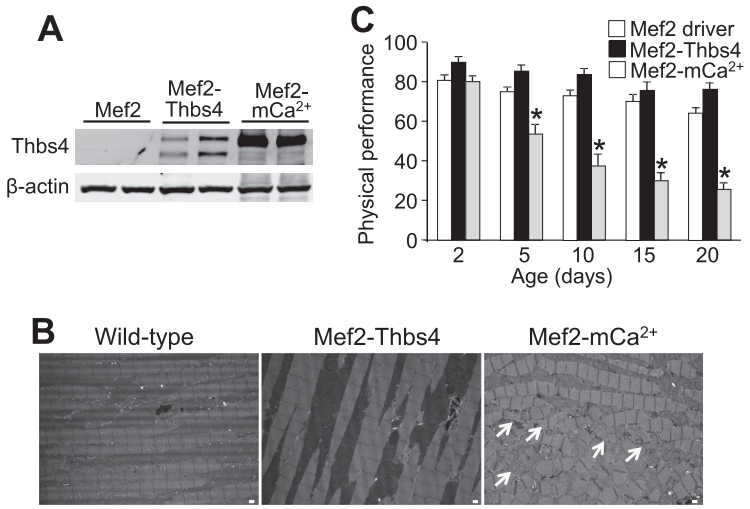

FIG 9 Transgenic *Drosophila* flies overexpressing the secretion-defective Thbs4 mutant have impaired muscle function. (A) Western blotting for Thbs4 expression in transgenic flies with Mef2-driven overexpression of wild-type Thbs4 (Mef2-Thbs4) or the secretion-defective mutant (Mef2-mCa^{2+}) or Mef2 driver alone as a negative control. (B) Electron microscopy of transgenic *Drosophila* of the indicated genotypes at 25 days of age for the indirect flight muscle. Arrows indicate torn regions of the muscle. Scale bar = 1 μm. (C) Negative-geotaxis assays were performed on transgenic flies of the indicated genotypes and ages to evaluate locomotor function. *, $P < 0.05$ versus the value for Mef2 driver control.

sarcoglycans and dystroglycans at the sarcolemma for greater membrane stability (11, 19, 29). In this study, we generated a Thbs4 mutant that is still capable of oligomerization and induction of the Atf6α-mediated ER stress pathway, expansion of intracellular vesicles, and acceleration of global anterograde trafficking toward the plasma membrane but is not secreted by cardiomyocytes. The secretion-defective mutant likely functions as a dominant negative protein that can bind Thbs4 substrates but not fully function as a chaperone for their trafficking through the secretory pathway with final secretion or membrane placement. Indeed, we observed decreased membrane localization of β-dystroglycan, β-sarcoglycan, and δ-sarcoglycan in hearts overexpressing the secretion-defective Thbs4 mutant. Moreover, we found accumulation of β-sarcoglycan at the Golgi apparatus in cardiomyocytes overexpressing secretion-deficient Thbs4. Thus, flux of Thbs4 through the secretory pathway is likely required for its chaperone-like activity toward enhancing the residency of dystroglycans, sarcoglycans, and likely other glycoproteins at the sarcolemma of cardiomyocytes and skeletal muscle myofibers. Despite accelerated intracellular vesicular trafficking caused by overexpression of the secretion-defective Thbs4 mutant, cardioprotection was not observed as is typically observed with wild-type Thbs4, but instead the mutant caused cardiomyopathy. Indeed, Atf6α activity alone expands the ER in skeletal muscle and cardiomyocytes and accelerates global secretory pathway flux, although this activity is not sufficient to increase trafficking of sarcolemmal glycoproteins to the myocyte plasma membrane and disease is not mitigated by enhanced Atf6α activity in dystrophic animal models (19, 29).

Proper content and localization of sarcoglycans and dystroglycans to the sarcolemma of cardiomyocytes and skeletal muscle myofibers are critical for maintaining sarcolemmal structural integrity (35, 39, 40). Dystroglycans and sarcoglycans are components of the dystrophin-glycoprotein complex (DGC), which serves as a vital anchoring system in myocyte membranes that protects against damage that typically underlies muscular dystrophy and cardiomyopathy (3–6). In skeletal muscle, Thbs4 overexpression profoundly enhanced membrane trafficking of integrins, dystroglycans, and sarcoglycans that was associated with protection from myofiber sarcolemmal damage (29). In this study, we observed that genetic inhibition of Thbs4 movement through the secretory pathway impairs trafficking and/or assembly of dystroglycans

and sarcoglycans at the sarcolemma. Indeed, similar to transgenic mice overexpressing the secretion-defective Thbs4 mutant in cardiomyocytes, mice with deletion of the cardiomyocyte-specific *Itgb1* (integrin β1) gene (41) and mice with genetically ablated dystroglycan glycosylation (42) have defects in cardiomyocyte membrane stability and develop cardiomyopathy. Moreover, genetic deletion of the sarcolemmal glycoprotein utrophin exacerbates cardiomyocyte damage in the *mdx* model of muscular dystrophy (43), which we also observed with deletion of *Thbs4* in *mdx* mice. These data suggest that enhancing residence of sarcolemmal glycoproteins may be an effective strategy in the treatment of cardiac disease in muscular dystrophy patients.

Thbs proteins are induced in cardiac and skeletal muscle during injury or disease (8, 10, 11, 29, 44, 45), which is likely a compensatory protective mechanism that increases membrane trafficking of integrins and DGC components to prevent mechanical load-induced sarcolemmal damage, as well as increase secretion of ECM proteins involved in healing and overall structural integrity. Importantly, heart failure is a leading cause of mortality in Duchenne muscular dystrophy and other muscular dystrophies (46–49), so therapeutic strategies that could bolster DGC complex stability at the plasma membrane with selectively enhanced ECM content in cardiomyocytes could potentially extend the life span of muscular dystrophy patients.

MATERIALS AND METHODS

Animals. Cardiac tissue-specific Thbs4 transgenic mice have been described previously (11). Mice with deletion of the *Thbs4* gene (stock 005845) and *mdx* mice (34) (stock 001801) were obtained from Jackson laboratories. Cardiac tissue-specific transgenic mice overexpressing the secretion-defective Thbs4 mutant (Thbs4-mCa^{2+}) containing mutations in six DXDXDG calcium binding motifs (D499/501/503A, D512/514/516A, D571/573/575A, D632/634/636A, D655/557/659A, and D668/670/672A) within the T3R domains of mouse Thbs4 were generated by subcloning the mCa^{2+} Thbs4 mutant cDNA from our previously generated adenoviral construct (19) into the α-myosin heavy chain promoter expression vector (31). The DNA construct was subjected to NotI restriction endonuclease digestion, gel purification of the promoter-cDNA fragment, and oocyte injection of this fragment through the Cincinnati Children's Hospital Transgenic Animal and Genome Editing Core Facility. *mdx* mice were on the C57/BL10 genetic background, *Thbs4*$^{-/-}$ mice were on the C57BL/6-SV129 background, and all transgenic mice were on the FVB/N background. Echocardiography was performed on anesthetized adult mice to noninvasively evaluate cardiac structure and function as described previously (50, 51). Transverse aortic constriction (TAC) to induce cardiac pressure overload was performed as described previously (50). All procedures were performed in accordance with the *Guide for the Care and Use of Laboratory Animals* (52) and approved by the Institutional Animal Care and Use Committee (IACUC) of Cincinnati Children's Hospital Medical Center.

Transgenic UAS-Thbs4 *Drosophila* flies were described previously (29). The secretion-defective Thbs4-mCa^{2+} cDNA was subcloned into the GAL4-responsive pUAST vector to generate transgenic UAS-Thbs4-mCa^{2+} *Drosophila* by P-element insertion (Rainbow Transgenics) into *y*^{1} *w*^{1118} embryos. Mef2-Gal4 driver *Drosophila* (Bloomington Stock Center, Indiana University) flies were used to induce Thbs4 expression in *Drosophila* muscle. Genotypes evaluated were *Mef2-Gal4*/+, UAS-*Thbs4*/+; *Mef2-Gal4*/+, and UAS-*Thbs4*-mCa^{2+}/+; *Mef2-Gal4*/+. Negative-geotaxis assays to evaluate locomotor function were performed exactly as described previously (29).

Cell culture, adenovirus transduction, and live cell imaging. Adenoviruses encoding β-galactosidase (Adβgal) and wild-type mouse Thbs4 or the secretion-defective Thbs4 Ca^{2+} binding mutant with a C-terminal Flag tag (19) and *Atf6*$^{-/-}$ mouse embryonic fibroblasts (MEFs) have been described previously (19, 53). Primary neonatal rat cardiomyocytes were isolated from 1- to 2-day-old Sprague-Dawley rat pups, cultured on gelatin-coated dishes as previously described (11), and maintained in M199 medium (Corning) supplemented with 1% bovine growth serum (BGS) (HyClone). Wild-type and *Atf6*$^{-/-}$ MEFs were cultured in Dulbecco modified Eagle medium (DMEM) (HyClone) supplemented with 10% BGS. Cells were transduced with adenovirus for 4 h and then given fresh medium. For electron microscopy studies, MEFs were harvested 72 h after adenovirus transduction. For immunoblotting of secreted proteins, 48 h after adenovirus transduction, cardiomyocytes were washed and put in fresh serum-free M199 medium. Culture medium was harvested 4 h later and concentrated in Amicon Ultra centrifugal filters (Millipore) by centrifugation at 5,000 $\times$ *g* for 30 min at 4°C, and Laemmli buffer was added to 30 μl of concentrated medium without boiling and loaded onto SDS-PAGEgel. Intracellular lysates were prepared for Western blotting from cardiomyocytes harvested from the culture dish as described below.

Evaluation of ER-to-Golgi and Golgi-to-plasma membrane vesicular trafficking was performed in neonatal rat cardiomyocytes by fluorescence recovery after photobleaching (FRAP) and inverse FRAP (iFRAP), respectively, exactly as described previously (29). Briefly, for FRAP experiments,cardiomyocytes were transduced with baculovirus encoding red fluorescent protein (RFP)-tagged *N*-acetylgalactosaminyltransferase (GalNAcT2-RFP) (CellLight Golgi-RFP Bacmam 2.0; Thermo Fisher) and treated with cycloheximide (100 μg/ml; Sigma), and a region of interest (ROI) in the perinuclear Golgi network was bleached with an argon laser. Recovery of the fluorescence signal was monitored

and quantified for live cardiomyocytes for 2 h to assess ER-to-Golgi trafficking. For iFRAP, cardiomyocytes were transduced with adenovirus encoding a temperature-sensitive VSVG-eGFP fusion protein, treated with cycloheximide, and incubated at 32°C to allow VSVG-eGFP to traffic to the Golgi apparatus. Then the entire cardiomyocyte was bleached with an argon laser and fluorescence in a region of interest including the perinuclear Golgi network was imaged for 2 h to quantify the reduction in fluorescence signal of VSVG-eGFP exiting the Golgi apparatus as a measure of Golgi-to-plasma membrane trafficking.

Western blotting and seminative PAGE. For seminative PAGE, cardiomyocyte lysates were harvested in Tris-buffered saline (TBS) with 1% *n*-dodecyl β-D-maltoside (DDM) with protease inhibitors (Roche), cleared by centrifugation, and prepared for SDS-PAGE by addition of 2× native PAGE sample buffer (62.5 mM Tris-HCl [pH 6.8], 40% glycerol, 0.01% bromophenol blue) without boiling. For immunoblotting of mouse cardiac or *Drosophila* proteins, mouse hearts or whole flies were homogenized in RIPA buffer (50 mM Tris-HCl [pH 7.4], 1% Triton X-100, 1% sodium deoxycholate, 1 mM EDTA, 0.1% SDS), sonicated, and cleared by centrifugation as described previously (50, 51).

For immunoprecipitation assays, cardiomyocyte lysates were harvested in TBS with 1% Triton X-100 with protease inhibitors (Roche) and immunoprecipitated with anti-Flag M2 magnetic beads (Sigma) overnight at 4°C. Immunoprecipitates were washed, boiled in Laemmli buffer, and analyzed by immunoblotting. Isolation of membrane glycoproteins was performed as described previously (54), with slight modifications. Mouse hearts were minced and incubated in solubilization buffer (phosphate-buffered saline [PBS], 0.1% digitonin, 0.5% Triton X-100) with protease inhibitors for 1 h at 4°C. Extracted proteins were clarified by centrifugation and glycoproteins were affinity purified by incubation of 2 mg of protein with wheat germ agglutinin-agarose (Vector Laboratories) for 1 h at 4°C. Isolated glycoproteins were then washed three times in solubilization buffer and eluted by boiling in Laemmli buffer. Proteins were resolved by SDS-PAGE, transferred to polyvinylidene difluoride (PVDF) membranes (Millipore), and immunoblotted with antibodies for Flag (Cell Signaling Technology or Sigma), calreticulin, PDI, integrin β1, pan-cadherin, and Rab6 (Cell Signaling Technology), Armet, SAR1, δ-sarcoglycan, and β-actin (Abcam), α-sarcoglycan and β-dystroglycan (Developmental Studies Hybridoma Bank), β-sarcoglycan (Novus Biologicals), Rab24 (BD Transduction), atrial natriuretic factor (ANF; Millipore), α-tubulin, BiP, and α-sarcomeric actin (Sigma), glyceraldehyde-3-phosphate dehydrogenase (GAPDH; Fitzgerald), and Thbs4 (Santa Cruz).

Immunohistochemistry, histology, and electron microscopy. Immunostaining experiments were performed as previously described (50, 51, 55). Briefly, paraformaldehyde-fixed paraffin-embedded cardiac sections were incubated in blocking solution (PBS, 5% goat serum, 1% bovine serum albumin [BSA], 1% glycine, 0.2% Triton X-100) for 1 h and then with anti-Thbs4 primary antibody (Santa Cruz) diluted 1:500 in blocking solution overnight, followed by incubation with Alexa Fluor-labeled secondary antibody (Invitrogen; 1:1,000) for 1 h. For immunocytochemistry, adult mouse cardiomyocytes were isolated from mouse hearts by Langendorff perfusion, fixed in 4% paraformaldehyde, and immunostained in suspension as described previously (51) using antibodies against β-sarcoglycan (Novus Biologicals) and GM130 (BD Biosciences) coupled to Alexa Fluor-labeled secondary antibodies (Invitrogen). Images were captured on a Nikon A1 confocal microscope.

Transmission electron microscopy (TEM) was performed as described elsewhere (19). MEFs or mouse hearts were fixed in glutaraldehyde-cacodylate buffer, embedded in epoxy resin, sectioned, and counterstained with lead citrate and uranyl acetate. *Drosophila* flies were processed for TEM exactly as described previously (29). Sections were imaged on a transmission electron microscope. Hematoxylin and eosin (H&E) staining of paraffin-embedded cardiac tissue sections was performed according to standard protocols as described previously (50, 51). Cell surface area (CSA) was measured in cardiac sections stained with wheat germ agglutinin-Alexa Fluor 488 conjugate (Thermo Fisher) using ImageJ (NIH) as described previously (50, 51). CSA was measured in at least 200 cardiomyocytes per animal, and the average CSAs of 3 to 6 animals per genotype were averaged. Terminal deoxynucleotidyltransferase-mediated dUTP-biotin nick end labeling (TUNEL) was performed on cardiac sections using an *in situ* cell death detection kit (Roche) according to the manufacturer's instructions.

Evans blue dye uptake. Mice were injected intraperitoneally with 100 mg/kg of Evans blue dye (EBD) diluted in PBS, and hearts were harvested 2 days later. Hearts were immediately embedded in OCT, frozen, cryosectioned, counterstained with wheat germ agglutinin-Alexa Fluor 488 conjugate (Thermo Fisher), and imaged by confocal microscopy, and EBD-positive cardiomyocytes were quantified as described previously (56). At least 2,000 cardiomyocytes were evaluated for EBD positivity per animal.

Statistical analysis. Statistical analysis was performed using Student's *t* test, except for data in Fig. 4C to E, for which one-way analysis of variance (ANOVA) with *post hoc* Turkey's test was used. Standard errors of the means are shown for averaged data.

ACKNOWLEDGMENTS

This work was supported by a National Research Service Award (F32HL124698) and Pathway to Independence Award (K99 HL136695) from the National Institutes of Health to M.J.B. and grants from the Howard Hughes Medical Institute and National Institutes of Health (R01HL105924) to J.D.M.

We declare no conflict of interest.

REFERENCES

1. Israeli-Rosenberg S, Manso AM, Okada H, Ross RS. 2014. Integrins and integrin-associated proteins in the cardiac myocyte. Circ Res 114:572–586. https://doi.org/10.1161/CIRCRESAHA.114.301275.
2. Brancaccio M, Hirsch E, Notte A, Selvetella G, Lembo G, Tarone G. 2006. Integrin signalling: the tug-of-war in heart hypertrophy. Cardiovasc Res 70:422–433. https://doi.org/10.1016/j.cardiores.2005.12.015.
3. Barresi R, Campbell KP. 2006. Dystroglycan: from biosynthesis to pathogenesis of human disease. J Cell Sci 119:199–207. https://doi.org/10.1242/jcs.02814.
4. Durbeej M, Campbell KP. 2002. Muscular dystrophies involving the dystrophin-glycoprotein complex: an overview of current mouse models. Curr Opin Genet Dev 12:349–361. https://doi.org/10.1016/S0959-437X(02)00309-X.
5. McGreevy JW, Hakim CH, McIntosh MA, Duan D. 2015. Animal models of Duchenne muscular dystrophy: from basic mechanisms to gene therapy. Dis Model Mech 8:195–213. https://doi.org/10.1242/dmm.018424.
6. Lapidos KA, Kakkar R, McNally EM. 2004. The dystrophin glycoprotein complex: signaling strength and integrity for the sarcolemma. Circ Res 94:1023–1031. https://doi.org/10.1161/01.RES.0000126574.61061.25.
7. Brody MJ, Lee Y. 2016. The role of leucine-rich repeat containing protein 10 (LRRC10) in dilated cardiomyopathy. Front Physiol 7:337. https://doi.org/10.3389/fphys.2016.00337.
8. Frolova EG, Sopko N, Blech L, Popovic ZB, Li J, Vasanji A, Drumm C, Krukovets I, Jain MK, Penn MS, Plow EF, Stenina OI. 2012. Thrombospondin-4 regulates fibrosis and remodeling of the myocardium in response to pressure overload. FASEB J 26:2363–2373. https://doi.org/10.1096/fj.11-190728.
9. Adams JC, Lawler J. 2011. The thrombospondins. Cold Spring Harb Perspect Biol 3:a009712. https://doi.org/10.1101/cshperspect.a009712.
10. Xia Y, Dobaczewski M, Gonzalez-Quesada C, Chen W, Biernacka A, Li N, Lee DW, Frangogiannis NG. 2011. Endogenous thrombospondin 1 protects the pressure-overloaded myocardium by modulating fibroblast phenotype and matrix metabolism. Hypertension 58:902–911. https://doi.org/10.1161/HYPERTENSIONAHA.111.175323.
11. Lynch JM, Maillet M, Vanhoutte D, Schloemer A, Sargent MA, Blair NS, Lynch KA, Okada T, Aronow BJ, Osinska H, Prywes R, Lorenz JN, Mori K, Lawler J, Robbins J, Molkentin JD. 2012. A thrombospondin-dependent pathway for a protective ER stress response. Cell 149:1257–1268. https://doi.org/10.1016/j.cell.2012.03.050.
12. Lawler J, Duquette M, Whittaker CA, Adams JC, McHenry K, DeSimone DW. 1993. Identification and characterization of thrombospondin-4, a new member of the thrombospondin gene family. J Cell Biol 120:1059–1067. https://doi.org/10.1083/jcb.120.4.1059.
13. Carlson CB, Lawler J, Mosher DF. 2008. Structures of thrombospondins. Cell Mol Life Sci 65:672–686. https://doi.org/10.1007/s00018-007-7484-1.
14. Adams JC, Lawler J. 2004. The thrombospondins. Int J Biochem Cell Biol 36:961–968. https://doi.org/10.1016/j.biocel.2004.01.004.
15. Chen TL, Posey KL, Hecht JT, Vertel BM. 2008. COMP mutations: domain-dependent relationship between abnormal chondrocyte trafficking and clinical PSACH and MED phenotypes. J Cell Biochem 103:778–787. https://doi.org/10.1002/jcb.21445.
16. Chen TL, Stevens JW, Cole WG, Hecht JT, Vertel BM. 2004. Cell-type specific trafficking of expressed mutant COMP in a cell culture model for PSACH. Matrix Biol 23:433–444. https://doi.org/10.1016/j.matbio.2004.09.005.
17. Hecht JT, Hayes E, Snuggs M, Decker G, Montufar-Solis D, Doege K, Mwalle F, Poole R, Stevens J, Duke PJ. 2001. Calreticulin, PDI, Grp94 and BiP chaperone proteins are associated with retained COMP in pseudoachondroplasia chondrocytes. Matrix Biol 20:251–262. https://doi.org/10.1016/S0945-053X(01)00136-6.
18. Vranka J, Mokashi A, Keene DR, Tufa S, Corson G, Sussman M, Horton WA, Maddox K, Sakai L, Bachinger HP. 2001. Selective intracellular retention of extracellular matrix proteins and chaperones associated with pseudoachondroplasia. Matrix Biol 20:439–450. https://doi.org/10.1016/S0945-053X(01)00148-2.
19. Brody MJ, Schips TG, Vanhoutte D, Kanisicak O, Karch J, Maliken BD, Blair NS, Sargent MA, Prasad V, Molkentin JD. 2016. Dissection of thrombospondin-4 domains involved in intracellular adaptive endoplasmic reticulum stress responsive signaling. Mol Cell Biol 36:2–12. https://doi.org/10.1128/MCB.00607-15.
20. Deere M, Sanford T, Francomano CA, Daniels K, Hecht JT. 1999. Identification of nine novel mutations in cartilage oligomeric matrix protein in patients with pseudoachondroplasia and multiple epiphyseal dysplasia. Am J Med Genet 85:486–490. https://doi.org/10.1002/(SICI)1096-8628(19990827)85:5<486::AID-AJMG10>3.0.CO;2-O.
21. Ikegawa S, Ohashi H, Nishimura G, Kim KC, Sannohe A, Kimizuka M, Fukushima Y, Nagai T, Nakamura Y. 1998. Novel and recurrent COMP (cartilage oligomeric matrix protein) mutations in pseudoachondroplasia and multiple epiphyseal dysplasia. Hum Genet 103:633–638. https://doi.org/10.1007/s004390050883.
22. Posey KL, Yang Y, Veerisetty AC, Sharan SK, Hecht JT. 2008. Model systems for studying skeletal dysplasias caused by TSP-5/COMP mutations. Cell Mol Life Sci 65:687–699. https://doi.org/10.1007/s00018-007-7485-0.
23. Carlson CB, Gunderson KA, Mosher DF. 2008. Mutations targeting intermodular interfaces or calcium binding destabilize the thrombospondin-2 signature domain. J Biol Chem 283:27089–27099. https://doi.org/10.1074/jbc.M803842200.
24. Hecht JT, Nelson LD, Crowder E, Wang Y, Elder FF, Harrison WR, Francomano CA, Prange CK, Lennon GG, Deere M, Lawler J. 1995. Mutations in exon 17B of cartilage oligomeric matrix protein (COMP) cause pseudoachondroplasia. Nat Genet 10:325–329. https://doi.org/10.1038/ng0795-325.
25. Briggs MD, Hoffman SM, King LM, Olsen AS, Mohrenweiser H, Leroy JG, Mortier GR, Rimoin DL, Lachman RS, Gaines ES, Cekleniak JA, Knowlton RG, Cohn DH. 1995. Pseudoachondroplasia and multiple epiphyseal dysplasia due to mutations in the cartilage oligomeric matrix protein gene. Nat Genet 10:330–336. https://doi.org/10.1038/ng0795-330.
26. Schmitz M, Niehoff A, Miosge N, Smyth N, Paulsson M, Zaucke F. 2008. Transgenic mice expressing D469Delta mutated cartilage oligomeric matrix protein (COMP) show growth plate abnormalities and sternal malformations. Matrix Biol 27:67–85. https://doi.org/10.1016/j.matbio.2007.08.001.
27. Hashimoto Y, Tomiyama T, Yamano Y, Mori H. 2003. Mutation (D472Y) in the type 3 repeat domain of cartilage oligomeric matrix protein affects its early vesicle trafficking in endoplasmic reticulum and induces apoptosis. Am J Pathol 163:101–110. https://doi.org/10.1016/S0002-9440(10)63634-6.
28. Kirk JA, Cingolani OH. 2016. Thrombospondins in the transition from myocardial infarction to heart failure. J Mol Cell Cardiol 90:102–110. https://doi.org/10.1016/j.yjmcc.2015.12.009.
29. Vanhoutte D, Schips TG, Kwong JQ, Davis J, Tjondrokoesoemo A, Brody MJ, Sargent MA, Kanisicak O, Hong Y, Gao QQ, Rabinowitz JE, Volk T, McNally EM, Molkentin JD. 2016. Thrombospondin expression in myofibers stabilizes muscle membranes. Elife 5:e17589. https://doi.org/10.7554/eLife.17589.
30. Wang S, Herndon ME, Ranganathan S, Godyna S, Lawler J, Argraves WS, Liau G. 2004. Internalization but not binding of thrombospondin-1 to low density lipoprotein receptor-related protein-1 requires heparan sulfate proteoglycans. J Cell Biochem 91:766–776. https://doi.org/10.1002/jcb.10781.
31. Sanbe A, Gulick J, Hanks MC, Liang Q, Osinska H, Robbins J. 2003. Reengineering inducible cardiac-specific transgenesis with an attenuated myosin heavy chain promoter. Circ Res 92:609–616. https://doi.org/10.1161/01.RES.0000065442.64694.9F.
32. Davis J, Maillet M, Miano JM, Molkentin JD. 2012. Lost in transgenesis: a user's guide for genetically manipulating the mouse in cardiac research. Circ Res 111:761–777. https://doi.org/10.1161/CIRCRESAHA.111.262717.
33. Matsuda R, Nishikawa A, Tanaka H. 1995. Visualization of dystrophic muscle fibers in mdx mouse by vital staining with Evans blue: evidence of apoptosis in dystrophin-deficient muscle. J Biochem 118:959–964. https://doi.org/10.1093/jb/118.5.959.
34. Bulfield G, Siller WG, Wight PA, Moore KJ. 1984. X chromosome-linked muscular dystrophy (mdx) in the mouse. Proc Natl Acad Sci U S A 81:1189–1192.
35. Yasuda S, Townsend D, Michele DE, Favre EG, Day SM, Metzger JM. 2005. Dystrophic heart failure blocked by membrane sealant poloxamer. Nature 436:1025–1029. https://doi.org/10.1038/nature03844.
36. Quinlan JG, Hahn HS, Wong BL, Lorenz JN, Wenisch AS, Levin LS. 2004. Evolution of the mdx mouse cardiomyopathy: physiological and morphological findings. Neuromuscul Disord 14:491–496. https://doi.org/10.1016/j.nmd.2004.04.007.

37. Khouzami L, Bourin MC, Christov C, Damy T, Escoubet B, Caramelle P, Perier M, Wahbi K, Meune C, Pavoine C, Pecker F. 2010. Delayed cardiomyopathy in dystrophin deficient mdx mice relies on intrinsic glutathione resource. Am J Pathol 177:1356–1364. https://doi.org/10.2353/ajpath.2010.090479.
38. Dahiya S, Givvimani S, Bhatnagar S, Qipshidze N, Tyagi SC, Kumar A. 2011. Osteopontin-stimulated expression of matrix metalloproteinase-9 causes cardiomyopathy in the mdx model of Duchenne muscular dystrophy. J Immunol 187:2723–2731. https://doi.org/10.4049/jimmunol.1101342.
39. Ervasti JM, Ohlendieck K, Kahl SD, Gaver MG, Campbell KP. 1990. Deficiency of a glycoprotein component of the dystrophin complex in dystrophic muscle. Nature 345:315–319. https://doi.org/10.1038/345315a0.
40. Mayer U, Saher G, Fassler R, Bornemann A, Echtermeyer F, von der Mark H, Miosge N, Poschl E, von der Mark K. 1997. Absence of integrin alpha 7 causes a novel form of muscular dystrophy. Nat Genet 17:318–323. https://doi.org/10.1038/ng1197-318.
41. Shai SY, Harpf AE, Babbitt CJ, Jordan MC, Fishbein MC, Chen J, Omura M, Leil TA, Becker KD, Jiang M, Smith DJ, Cherry SR, Loftus JC, Ross RS. 2002. Cardiac myocyte-specific excision of the beta1 integrin gene results in myocardial fibrosis and cardiac failure. Circ Res 90:458–464. https://doi.org/10.1161/hh0402.105790.
42. Michele DE, Kabaeva Z, Davis SL, Weiss RM, Campbell KP. 2009. Dystroglycan matrix receptor function in cardiac myocytes is important for limiting activity-induced myocardial damage. Circ Res 105:984–993. https://doi.org/10.1161/CIRCRESAHA.109.199489.
43. Grady RM, Teng H, Nichol MC, Cunningham JC, Wilkinson RS, Sanes JR. 1997. Skeletal and cardiac myopathies in mice lacking utrophin and dystrophin: a model for Duchenne muscular dystrophy. Cell 90:729–738. https://doi.org/10.1016/S0092-8674(00)80533-4.
44. Frangogiannis NG, Ren G, Dewald O, Zymek P, Haudek S, Koerting A, Winkelmann K, Michael LH, Lawler J, Entman ML. 2005. Critical role of endogenous thrombospondin-1 in preventing expansion of healing myocardial infarcts. Circulation 111:2935–2942. https://doi.org/10.1161/CIRCULATIONAHA.104.510354.
45. Cingolani OH, Kirk JA, Seo K, Koitabashi N, Lee DI, Ramirez-Correa G, Bedja D, Barth AS, Moens AL, Kass DA. 2011. Thrombospondin-4 is required for stretch-mediated contractility augmentation in cardiac muscle. Circ Res 109:1410–1414. https://doi.org/10.1161/CIRCRESAHA.111.256743.
46. Judge DP, Kass DA, Thompson WR, Wagner KR. 2011. Pathophysiology and therapy of cardiac dysfunction in Duchenne muscular dystrophy. Am J Cardiovasc Drugs 11:287–294. https://doi.org/10.2165/11594070-000000000-00000.
47. Finsterer J, Stollberger C. 2003. The heart in human dystrophinopathies. Cardiology 99:1–19. https://doi.org/10.1159/000068446.
48. Van Ruiten HJ, Marini Bettolo C, Cheetham T, Eagle M, Lochmuller H, Straub V, Bushby K, Guglieri M. 2016. Why are some patients with Duchenne muscular dystrophy dying young: an analysis of causes of death in North East England. Eur J Paediatr Neurol 20:904–909. https://doi.org/10.1016/j.ejpn.2016.07.020.
49. Mavrogeni S, Markousis-Mavrogenis G, Papavasiliou A, Kolovou G. 2015. Cardiac involvement in Duchenne and Becker muscular dystrophy. World J Cardiol 7:410–414. https://doi.org/10.4330/wjc.v7.i7.410.
50. Brody MJ, Feng L, Grimes AC, Hacker TA, Olson TM, Kamp TJ, Balijepalli RC, Lee Y. 2016. LRRC10 is required to maintain cardiac function in response to pressure overload. Am J Physiol Heart Circ Physiol 310:H269–H278. https://doi.org/10.1152/ajpheart.00717.2014.
51. Brody MJ, Hacker TA, Patel JR, Feng L, Sadoshima J, Tevosian SG, Balijepalli RC, Moss RL, Lee Y. 2012. Ablation of the cardiac-specific gene leucine-rich repeat containing 10 (lrrc10) results in dilated cardiomyopathy. PLoS One 7:e51621. https://doi.org/10.1371/journal.pone.0051621.
52. National Research Council. 2011. Guide for the care and use of laboratory animals, 8th ed. National Academies Press, Washington, DC.
53. Yamamoto K, Sato T, Matsui T, Sato M, Okada T, Yoshida H, Harada A, Mori K. 2007. Transcriptional induction of mammalian ER quality control proteins is mediated by single or combined action of ATF6alpha and XBP1. Dev Cell 13:365–376. https://doi.org/10.1016/j.devcel.2007.07.018.
54. Campbell KP, Kahl SD. 1989. Association of dystrophin and an integral membrane glycoprotein. Nature 338:259–262. https://doi.org/10.1038/338259a0.
55. Brody MJ, Cho E, Mysliwiec MR, Kim TG, Carlson CD, Lee KH, Lee Y. 2013. Lrrc10 is a novel cardiac-specific target gene of Nkx2-5 and GATA4. J Mol Cell Cardiol 62:237–246. https://doi.org/10.1016/j.yjmcc.2013.05.020.
56. Wallner M, Duran JM, Mohsin S, Troupes CD, Vanhoutte D, Borghetti G, Vagnozzi RJ, Gross P, Yu D, Trappanese DM, Kubo H, Toib A, TESharp 3rd, Harper SC, Volkert MA, Starosta T, Feldsott EA, Berretta RM, Wang T, Barbe MF, Molkentin JD, Houser SR. 2016. Acute catecholamine exposure causes reversible myocyte injury without cardiac regeneration. Circ Res 119:865–879. https://doi.org/10.1161/CIRCRESAHA.116.308687.